Cdk2 loss accelerates precursor differentiation and remyelination in the adult central nervous system

Céline Caillava,[1,2,3] Renaud Vandenbosch,[4] Beata Jablonska,[5] Cyrille Deboux,[1,2,3] Giulia Spigoni,[1,2,3] Vittorio Gallo,[5] Brigitte Malgrange,[4] and Anne Baron-Van Evercooren[1,2,3,6]

[1]UMR-S975, Centre de Recherche de l'Institut du Cerveau et de la Moelle Epinière, Université Pierre et Marie Curie-Paris 6, Paris 75013, France
[2]U975, Institut National de la Santé et de la Recherche Médicale, Paris 75013, France
[3]UMR 7225, Centre National de la Recherche Scientifique, Paris 75013, France
[4]Developmental Neurobiology Unit, GIGA-Neurosciences, Centre Hospitalier Universitaire de Liège, Domaine Universitaire du Sart Tilman, 4000 Liège, Belgium
[5]Children's National Medical Center, Center for Neuroscience Research, Washington DC 20010
[6]Assistance Publique Hopitaux De Paris, Hôpital Pitié-Salpêtrière, Fédération de Neurologie Paris 75013, France

The specific functions of intrinsic regulators of oligodendrocyte progenitor cell (OPC) division are poorly understood. Type 2 cyclin-dependent kinase (Cdk2) controls cell cycle progression of OPCs, but whether it acts during myelination and repair of demyelinating lesions remains unexplored. Here, we took advantage of a viable $Cdk2^{-/-}$ mutant mouse to investigate the function of this cell cycle regulator in OPC proliferation and differentiation in normal and pathological conditions. During central nervous system (CNS) development, Cdk2 loss does not affect OPC cell cycle, oligodendrocyte cell numbers, or myelination. However, in response to CNS demyelination, it clearly alters adult OPC renewal, cell cycle exit, and differentiation. Importantly, Cdk2 loss accelerates CNS remyelination of demyelinated axons. Thus, Cdk2 is dispensable for myelination but is important for adult OPC renewal, and could be one of the underlying mechanisms that drive adult progenitors to differentiate and thus regenerate myelin.

Introduction

Cell proliferation is a key phenomenon during development and repair. It is regulated by complex extrinsic and intrinsic mechanisms involving Cdks, a family of serine/threonine kinases that represents the core of the cell cycle machinery. Successive waves of Cdk activity control initiation and progression through the eukaryotic cell cycle in response to both intracellular and extracellular signals. During G1 phase, phosphorylation of the retinoblastoma protein (Rb) by Cdk4/6 and Cdk2—activated upon specific binding of the D and E cyclins, respectively (Morgan, 1997)—promotes transcription of genes essential for S phase entry. Activity of Cdk2/cyclin E complexes is thought to irreversibly phosphorylate Rb proteins to promote G1/S transition.

Despite the fundamental role of Cdks in cell cycle progression, recent data demonstrated molecular redundancies in their function, as single targeted disruption of mouse *Cdk2*, *Cdk4*, or *Cdk6* genes did not result in lethality, nor in defects in organogenesis (Rane et al., 1999; Tsutsui et al., 1999; Berthet et al., 2003; Ortega et al., 2003; Malumbres et al., 2004). However, inactivation of genes encoding individual Cdks affects cell division in specific cell types (Rane et al., 1999; Tsutsui et al., 1999; Moons et al., 2002; Malumbres et al., 2004; Atanasoski et al., 2008; Lange et al., 2009). In spite of its crucial role in the cell cycle, and probably because of redundancies with other Cdks, Cdk2 was shown to be dispensable during embryonic development, as Cdk2-null mice are viable, but indispensable in specific cell types, as Cdk2-null mice are sterile (Berthet et al., 2003).

In the central nervous system (CNS), proliferation of oligodendrocyte progenitor cells (OPCs) is crucial for effective myelination and remyelination. Indeed, during development, the majority of OPCs undergo a limited period of proliferation, before cell cycle exit and terminal differentiation into myelinating oligodendrocytes (Temple and Raff, 1986). However, a

Correspondence to Anne Baron-Van Evercooren: anne.baron@upmc.fr

Abbreviations used in this paper: ASVZ, anterior SVZ; CC, corpus callosum; CNS, central nervous system; dpi, days postinjection; GFAP, glial fibrillary acidic protein; KO, knockout; LPC, lysolecithin; MBP, myelin basic protein; NPC, neural precursor cell; OPC, oligodendrocyte progenitor cell; PSA-NCAM, polysialated neural cell adhesion molecule; RMS, rostral migratory stream; SVZ, subventricular zone; WT, wild type.

The Rockefeller University Press $30.00
J. Cell Biol. Vol. 193 No. 2 397–407
www.jcb.org/cgi/doi/10.1083/jcb.201004146

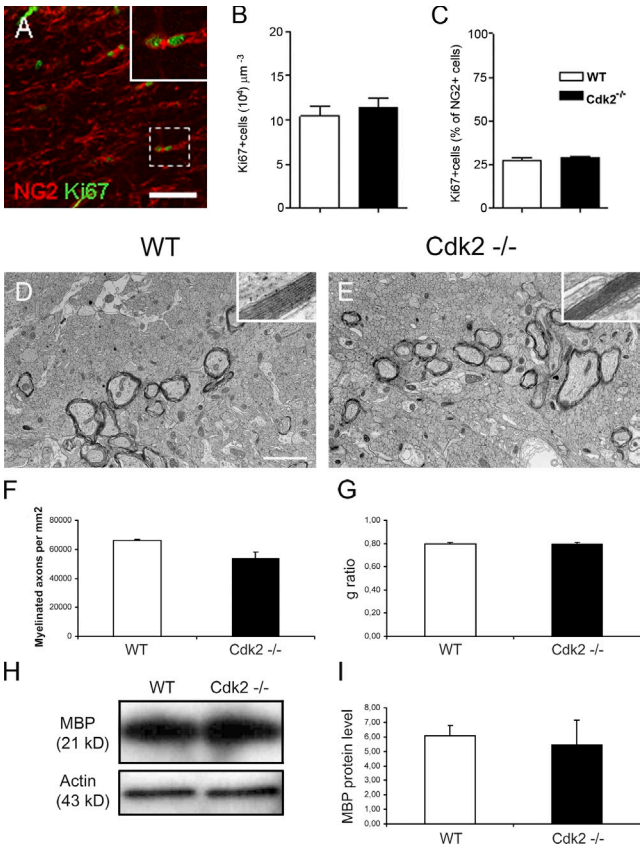

Figure 1. **OPC proliferation and postnatal myelination in Cdk2$^{-/-}$ mice.** (A) Coronal section of the CC area from P8 WT mice immunostained for NG2 and Ki67. Inset (enlarged view of the boxed region) identifies double-labeled cells. Bar, 50 µm. (B) Histogram comparing the overall density of Ki67^{+} cells in the CC at P8 in WT versus Cdk2$^{-/-}$ mice. (C) Histogram comparing the proliferative rate of NG2-expressing OPCs at P8 in WT versus Cdk2$^{-/-}$ mice. (D and E) Images of the CC were taken by electron microscopy from ultrathin sections of WT (D) and Cdk2$^{-/-}$ (E) P15 mice. The myelin sheath is represented at a higher magnification in the inset. Bar, 2 µm. (F) Histogram representing the number of myelinated axons in the CC. (G) Histogram representing g ratio in WT versus Cdk2$^{-/-}$ mice. (H and I) Western blot analysis of MBP quantity in WT versus Cdk2$^{-/-}$ mice. Actin was used as a loading control. Results are expressed as means ± SEM (error bars) and were analyzed by a *t* test.

population of slowly dividing OPCs persists throughout the adult CNS (Ffrench-Constant and Raff, 1986; Wolswijk and Noble, 1989; Reynolds and Hardy, 1997). Despite their low oligodendrogenic potential under physiological conditions, adult OPCs are responsible for remyelination after white matter insults (Wolswijk and Noble, 1989; Gensert and Goldman, 1997; Chang et al., 2000; Franklin, 2002). OPCs can also be generated by neural precursor cells (NPCs) of the subventricular zone (SVZ) in the adult forebrain both under physiological conditions (Levison and Goldman, 1993; Doetsch et al., 1999) and after demyelination in rodents and human brain (Nait-Oumesmar et al., 1999; Picard-Riera et al., 2002; Nait-Oumesmar et al., 2007). After demyelination of the adult brain, SVZ-derived OPCs are recruited to the lesions and contribute to remyelination (Menn et al., 2006; Aguirre et al., 2007).

CNS myelination and remyelination result from coordinated spatio-temporal events involving OPC proliferation, migration/recruitment, and differentiation into functional myelin-competent cells. Thus, these developmental-repair processes appear to be ideal events to investigate the requirements for Cdk2 in NPC/OPC cell cycle regulation. Although previous studies showed that Cdk2 controls cell cycle progression of neonatal OPCs in vitro (Belachew et al., 2002), and proliferation and self-renewal of adult NPCs (Jablonska et al., 2007), the role of this Cdk in NPC/OPC cell cycle regulation in pathological conditions has not yet been investigated.

In the present study, we have used Cdk2 knockout (KO) mice to investigate the role of Cdk2 in adult OPC and NPC proliferation and differentiation in vivo, and to demonstrate its implication in oligodendrocyte regeneration and remyelination in the white matter under pathological conditions. Because myelin is essential for axonal conduction, neuroprotection, and fine-tuning of brain signals during neural development and brain repair (Fields, 2008), our study defines an important molecular mechanism that regulates a crucial regenerative process in the mammalian brain.

Results

Cdk2 loss alters neither OPC proliferation nor developmental myelination in the postnatal and adult corpus callosum

Cdk2 is considered a key regulator of S phase entry and a crucial mediator of OPC cell cycle progression in vitro (Belachew et al., 2002). To identify a possible requirement of Cdk2 in dividing cells of the corpus callosum (CC) in vivo, we first quantified the total number of proliferating Ki67^{+} cells at P8 and P90. As described previously (Belachew et al., 2002), we observed a dramatic developmental reduction (>90%) of the number of Ki67^{+} cells between P8 and P90 (Fig. 1 B and Fig. S2 B), but no significant difference was detected between genotypes (wild type [WT] vs. Cdk2$^{-/-}$; Fig. 1 B and Fig. S2 B). Double immunohistochemistry for NG2, a marker of OPCs, and Ki67 confirmed previously observed differences in proliferation of NG2^{+} cells in the adult anterior SVZ and in the rostral migratory stream (Fig. S2 C; Jablonska et al., 2007). However, no alteration in the proliferating fraction of NG2^{+} cells at P8 (Fig. 1, A and C) or at P90 (Fig. S2 C) was observed in the CC of mutant versus control animals. These results suggest that, in vivo, OPC proliferation in the CC during early postnatal and adult stages is either Cdk2 independent or efficiently compensated by other Cdks.

Throughout early postnatal and adult life, white matter oligodendrocytes derive from OPCs that undergo a series of developmental changes before acquiring a mature phenotype (Pfeiffer et al., 1993). Specific markers characterize consecutive stages of oligodendrocyte maturation. Among various markers, NG2 labels OPCs and CC1 is a marker of postmitotic oligodendrocytes; conversely, Olig2 is expressed through the entire oligodendroglial lineage (Zhou et al., 2000). Given that OPC proliferation was not altered in Cdk2$^{-/-}$ mice, we observed no change in the densities of the different oligodendrocyte populations in WT versus Cdk2$^{-/-}$ mice at any developmental stage examined (Fig. S1).

We demonstrated that Cdk2 loss does not affect the number of oligodendrocytes and OPCs or their proliferation rate.

However, as in the CNS oligodendrocytes are responsible for myelin sheath synthesis, with each cell myelinating up to 40 independent axonal segments (Matthews and Duncan, 1971), loss of Cdk2 could impact myelin synthesis. To investigate this possibility, we used electron microscopy to quantify numbers of myelinated axons in the CC at postnatal day 15 (P15), a period of active myelination in rodents. We did not observe any difference in the numbers of myelinated axons in the CC between WT and Cdk2$^{-/-}$ mice (Fig. 1, D–F). In addition, Western blot quantification of myelin basic protein (MBP), one of the most abundant CNS myelin protein (Boggs, 2006), showed no difference in its level between the two genotypes (Fig. 1, H and I). Despite these findings, we questioned whether loss of Cdk2 could impact myelin sheath structure. High-magnification ultrastructural analysis showed that myelin sheath appearance was normal in the absence of Cdk2 (Fig. 1, D and E, insets). Furthermore, g ratio assessment indicated similar myelin thickness in Cdk2$^{-/-}$ and WT mice (Fig. 1 G). Finally, no differences in the parameters described above were observed between Cdk2$^{-/-}$ and WT mice at later stages of the myelination process in the adult brain (P90; Fig. S2, D–I). We also confirmed that the total number of axons was not significantly different between the two genotypes (WT, 991,128 ± 44,190 axons/mm^2; Cdk2$^{-/-}$, 914,113 ± 26,150 axons/mm^2; P = 0.14; results were analyzed with a *t* test).

Loss of Cdk2 attenuates cell proliferation in response to demyelination in the adult brain

Demyelination of the CC is known to increase proliferation of NPCs in the adult SVZ (Nait-Oumesmar et al., 1999; Decker et al., 2002). Thus, we investigated the role of Cdk2 in cell proliferation in the adult anterior SVZ (ASVZ), where stem cells and neural progenitors proliferate, and in the rostral migratory stream (RMS), where cells migrate toward the olfactory bulb. We compared proliferation in adult (P90) Cdk2$^{-/-}$ and WT mice in response to demyelination. Adult mice were injected with lysolecithin (LPC) to induce focal demyelination in the rostral CC (Fig. S3 D) and were sacrificed 7 d postinjection (dpi). In this well-established animal model (Nait-Oumesmar et al., 1999; Woodruff and Franklin, 1999; Watanabe et al., 2002), demyelination is accomplished within 2 d after toxin injection, and a proliferative cellular response is observed in both the ASVZ/RMS and the lesion (Nait-Oumesmar et al., 1999) during the first week after LPC injection.

We first quantified the rate of cell proliferation in response to demyelination by using Ki67 immunostaining, and found that, as previously demonstrated in the absence of demyelination (Fig. S2 C; Jablonska et al., 2007), the absence of Cdk2 induced a significant decrease in the total number of proliferating cells of the ASVZ and RMS (Fig. 2, A, B, and D). We next evaluated whether Cdk2 influences OPC proliferation in the demyelinated lesion. At 7 dpi, the lesion area was defined by the absence of MBP labeling. No difference in lesion size could be found between Cdk2$^{-/-}$ and WT animals (WT, 0.58 ± 0.09 mm^2 of demyelinated area; Cdk2$^{-/-}$, 0.49 ± 0.08 mm^2; P = 0.46; results were analyzed with a *t* test). Although the loss of Cdk2 had no effect on proliferation in the CC of nonlesioned mice (Fig. S2B), we found that the number of proliferative Ki67$^+$ cells in the lesion was significantly decreased in Cdk2$^{-/-}$ mutants, as compared with WT mice (Fig. 2, C and D). These results were also confirmed by evaluating cell proliferation using BrdU incorporation, which identifies cells progressing through S phase (Fig. S3).

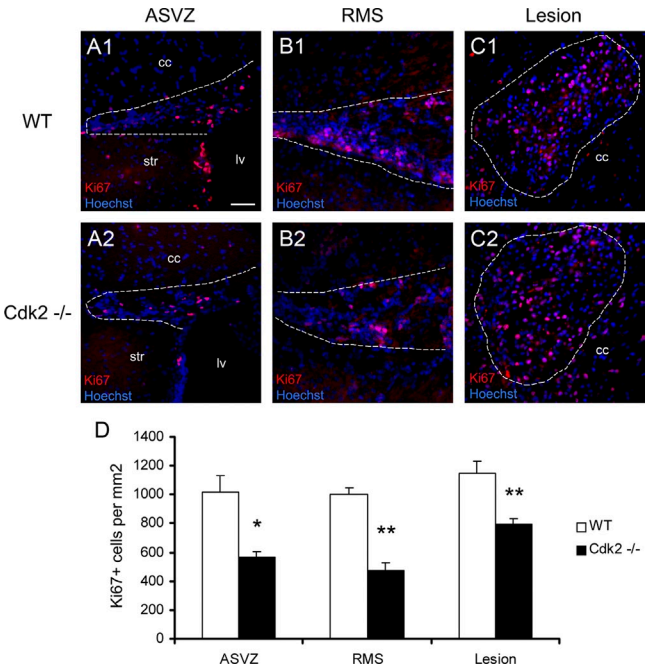

Figure 2. **Cell proliferation in response to demyelination in the adult brain.** (A–C) 7 dpi, proliferating cells were labeled with anti-Ki67 in the ASVZ (A), the RMS (B), and in the demyelinated lesion (C) of WT (A1–C1) and Cdk2$^{-/-}$ P90 mice (A2–C2). Broken lines delineate the different regions. cc, corpus callosum; str, striatum; lv, lateral ventricle. Bar, 50 µm. (D) Histogram representing the number of Ki67 labeled cells per surface in each region. Results are expressed as means ± SEM (error bars; *, P < 0.05; **, P < 0.001) and were analyzed by a *t* test.

Because the decrease in proliferation observed in different structures of Cdk2$^{-/-}$ brains could be caused by an increase in cell death in response to demyelination, we also investigated the potential contribution of apoptosis. TUNEL$^+$ cells were quantified in different brain regions (ASVZ/RMS, CC, and lesion) after LPC demyelination. No significant difference was observed in the rate of cell death between Cdk2$^{-/-}$ and WT mice (Fig. S4).

Finally, we also compared cell cycle exit of Olig2$^+$ oligodendroglial lineage cells in Cdk2$^{-/-}$ versus WT mice. BrdU was injected 15 h before sacrifice. As BrdU labels a cohort of cells in S phase, and Ki67 labels proliferating cells throughout all phases of the cell cycle, double-immunoreactive BrdU$^+$/Ki67$^+$ cells measured the proportion of cycling cells, whereas the remaining BrdU$^+$/Ki67$^-$ cells indicated cells that exited from the cell cycle. The cell cycle exit index of Olig2$^+$ cells (number of Olig2$^+$/BrdU$^+$/Ki67$^-$ cells divided by the total population of Olig2$^+$/BrdU$^+$ cells) showed that loss of Cdk2 caused a significant increase in Olig2$^+$ cell cycle exit in both the SVZ and the demyelinated lesion (Fig. 3).

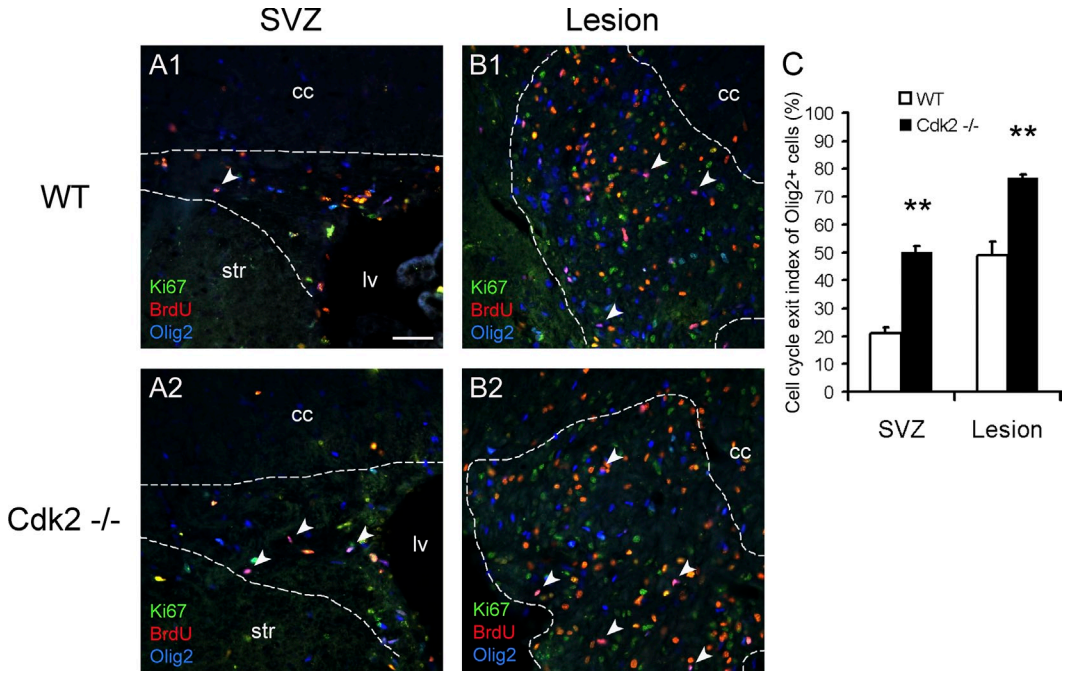

Figure 3. **Cell cycle exit in response to demyelination in the adult brain.** (A and B) 7 d after LPC injection, cells were labeled with anti-Olig2, anti-BrdU, and anti-Ki67 in the ASVZ (A) and in the demyelinated lesion (B) of WT (A1–B1) and Cdk2$^{-/-}$ P90 mice (A2–B2). As BrdU was injected 15 h before sacrifice, triple-immunoreactive Olig2$^+$/BrdU$^+$/Ki67$^+$ cells measured the proportion of Olig2$^+$ cycling cells while the remaining Olig2$^+$/BrdU$^+$/Ki67$^-$ cells indicated Olig2$^+$ cells that exited from the cell cycle. Broken lines delineate the different regions. Arrowheads point to double-labeled cells Olig2$^+$/BrdU$^+$/Ki67$^-$. cc, corpus callosum; str, striatum; lv, lateral ventricle. Bar, 50 µm. (C) Histogram representing the cell cycle exit index of Olig2$^+$ cells calculated by dividing the number of Olig2$^+$/BrdU$^+$/Ki67$^-$ cells by the total population of Olig2$^+$/BrdU$^+$ cells. Results are expressed as means ± SEM (error bars; **, $P < 0.001$) and were analyzed by a *t* test.

Cdk2 loss affects proliferation of specific ASVZ cell types in response to demyelination

In the adult SVZ, slowly dividing stem cells (type B cells) expressing glial fibrillary acidic protein (GFAP) and nestin give rise to highly proliferative transient-amplifying cells (type C cells), which express Mash1, Dlx2, and/or Olig2. These cells differentiate into migrating neuroblasts (type A cells) expressing the polysialylated acidic form of the neural cell adhesion molecule (PSA-NCAM), class III β-tubulin (Tuj1), or doublecortin (Dcx; Doetsch et al., 2002). Type B cells also generate other SVZ progenitors expressing NG2, which are highly proliferative type C–like cells and give rise mainly to oligodendrocytes (Nishiyama, 1998; Aguirre et al., 2004; Cerghet et al., 2006; Nishiyama, 2007). To identify which cell population of the ASVZ was mostly affected by the loss of Cdk2 in response to demyelination, we performed immunohistochemical analysis at 7 dpi using the proliferation marker Ki67 and BrdU, in combination with specific markers of each cell type (Fig. 4 and Fig. S5). Quantification of double-labeled cells showed that Cdk2 loss had no effect on the proliferative potential of GFAP$^+$ cells in response to demyelination (Fig. S5 A). This is consistent with the very low rate of proliferation of these stem cells, and previous results obtained in normal, nondemyelinated brains (Jablonska et al., 2007). Proliferation of PSA-NCAM$^+$ cells was also unaffected by Cdk2 loss (Fig. S5 B). However, Cdk2 loss induced a significant twofold decrease in the proliferation rate of cells giving rise to oligodendrocytes in response to demyelination, including NG2$^+$, Olig2$^+$, and Mash1$^+$ cells (Fig. 4, A, B, and C; Gensert and Goldman, 1997; Watanabe et al., 2002; Menn et al., 2006; Parras et al., 2007).

Loss of Cdk2 specifically affects oligodendrocyte proliferation in LPC lesions

Multiple cell types proliferate in response to LPC-induced demyelination, particularly astrocytes and oligodendrocytes. Furthermore, although the immune response is reduced in the LPC focal demyelination model, as compared with experimental autoimmune encephalomyelitis, microglia/macrophages still play a major role in eliminating myelin fragments. To examine the consequence of Cdk2 loss in proliferation on various glial cell populations after demyelination, we performed immunohistochemical analysis using the proliferation marker Ki67 in combination with specific cellular markers (Fig. 5). In the lesion, loss of Cdk2 did not affect proliferation of CD45$^+$ cells, a general marker for immune cells or GFAP$^+$ astrocytes (Fig. 5, A and B). However, the absence of Cdk2 specifically altered oligodendrocyte proliferation, as proliferation of the Olig2$^+$ oligodendroglial population (Fig. 5 C) and of the NG2$^+$ OPC pool (Fig. 5 D) were both significantly decreased when compared with WT littermates at 7 dpi. To better define the dynamics of OPC proliferation, we also analyzed proliferation of these cells at 14 dpi. As predicted from the well-defined profile of cellular dynamics during demyelination and remyelination in LPC lesions (Nait-Oumesmar et al., 1999; Woodruff and Franklin, 1999; Watanabe et al., 2002; Aguirre et al., 2007), we observed

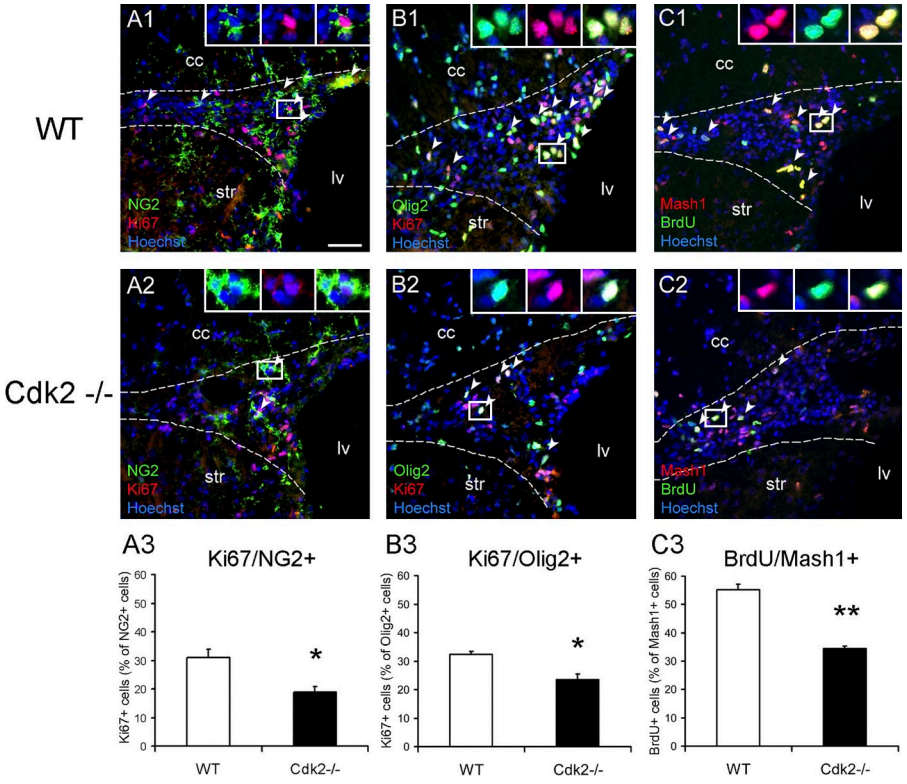

Figure 4. **Characterization of adult ASVZ cells in which proliferation is affected by the loss of Cdk2 in response to demyelination.** Characterization of proliferating cells in the ASVZ (cc, corpus callosum; str, striatum; lv, lateral ventricle) on sagittal sections obtained from WT (A1–C1) and Cdk2$^{-/-}$ (A2–C2) P90 mice at 7 dpi. Sections are stained with anti-Ki67 or anti-BrdU and a marker specific for different ASVZ cell types: NG2 (A1–2), Olig2 (B1–2), and Mash1 (C1–2). Broken lines delineate the ASVZ. Arrowheads point to double-labeled cells. Cells in the boxed areas are represented with threefold magnification in the inset. Bar, 50 µm. (A3–C3) Histograms representing the number of proliferating cells of each type in the ASVZ in response to demyelination. Results are expressed as means ± SEM (error bars; *, $P < 0.05$; **, $P < 0.001$) and were analyzed by a *t* test.

a high rate OPC proliferation in WT mice in response to demyelination at 7 dpi, followed by a decrease at 14 dpi corresponding to the differentiation phase (Fig. 5 D). Interestingly, Cdk2$^{-/-}$ OPC proliferation remained at steady levels at 14 dpi compared with 7 dpi (Fig. 5 D), which suggests that Cdk2$^{-/-}$ OPCs are less responsive to the lesion-induced signals of proliferation.

Oligodendrocyte maturation is accelerated in the absence of Cdk2

In CC, two sources of cells are likely to contribute to endogenous remyelination: the resident white matter adult OPCs and stem/precursor cells migrating from the adult SVZ (Gensert and Goldman, 1997; Nait-Oumesmar et al., 1999; Picard-Riera et al., 2002; Watanabe et al., 2002; Menn et al., 2006; Aguirre et al., 2007). Given the effect of Cdk2 loss on OPC proliferation in these two areas, we also investigated its impact on oligodendrocyte differentiation in the lesion. In rodents, spontaneous remyelination begins at 7 dpi and proceeds to be completed after 28 dpi. At 7 dpi, the density of Olig2$^+$ cells in the lesion was similar in Cdk2$^{-/-}$ and WT animals, and resulted from a slightly higher density of CC1$^+$ cells and a reduced density of NG2$^+$ cells (Fig. 6 D) in Cdk2$^{-/-}$ mice, as compared with WT, which indicates a decreased number of immature cells in Cdk2$^{-/-}$. At 14 dpi, both the density of Olig2$^+$ cells and the density of NG2$^+$ OPCs in the lesion were reduced in Cdk2$^{-/-}$ mice, as compared with WT (Fig. 6, A, C, and E). However, the density of CC1$^+$ cells was significantly increased in the lesion of Cdk2$^{-/-}$ mice (Fig. 6, B and E) compared with WT, which indicates enhanced differentiation of immature OPCs to mature oligodendrocytes. These findings were consistent with the lower proliferation rate of these cell populations in the Cdk2$^{-/-}$ mouse.

To better define the dynamics of oligodendroglial differentiation in the lesion, the same cell markers were also analyzed 21 dpi, i.e., when the population of oligodendrocytes is likely to have matured. In the absence of Cdk2, the density of Olig2$^+$ cells and NG2$^+$ cells remained lower than in WT (Fig. 6 F). However, the density of CC1$^+$ cells was similar in Cdk2$^{-/-}$ and WT mice. These results suggest that, in the absence of Cdk2, the rate of oligodendrocyte differentiation was accelerated during the process of remyelination, but the delay of differentiation observed in WT compared with Cdk2$^{-/-}$ mice recovered with time.

Accelerated differentiation of adult OPCs in the absence of Cdk2 was further analyzed in OPCs purified from adult Cdk2$^{-/-}$ and WT mice grown for 5 d in vitro. Immunohistochemistry for A2B5 (a marker for OPCs) and O4 (a marker of preoligodendrocytes) showed that, after 5 d in vitro, the number of immature A2B5$^+$ cells was reduced threefold in Cdk2$^{-/-}$ oligodendroglial cultures, as compared with WT cells (Fig. 7, A, B, and E). In contrast, the number of O4$^+$ preoligodendrocytes was significantly increased, and these cells displayed a more branched morphology in the absence of Cdk2, as compared with controls (Fig. 7, C–F), although the initial number of O4$^+$ cells (5 h after plating) was identical (WT, 8 ± 1%; Cdk2$^{-/-}$, 13 ± 2%; $P = 0.14$, results were analyzed with a *t* test). Similar data were also obtained for GalC$^+$ cells.

Remyelination is accelerated in the lesions of Cdk2 KO mice

We further investigated if the accelerated oligodendrocyte differentiation observed in the absence of Cdk2 had an impact on remyelination. Electron microscopy analysis of ultrathin sections was used to precisely quantify the number of myelinated

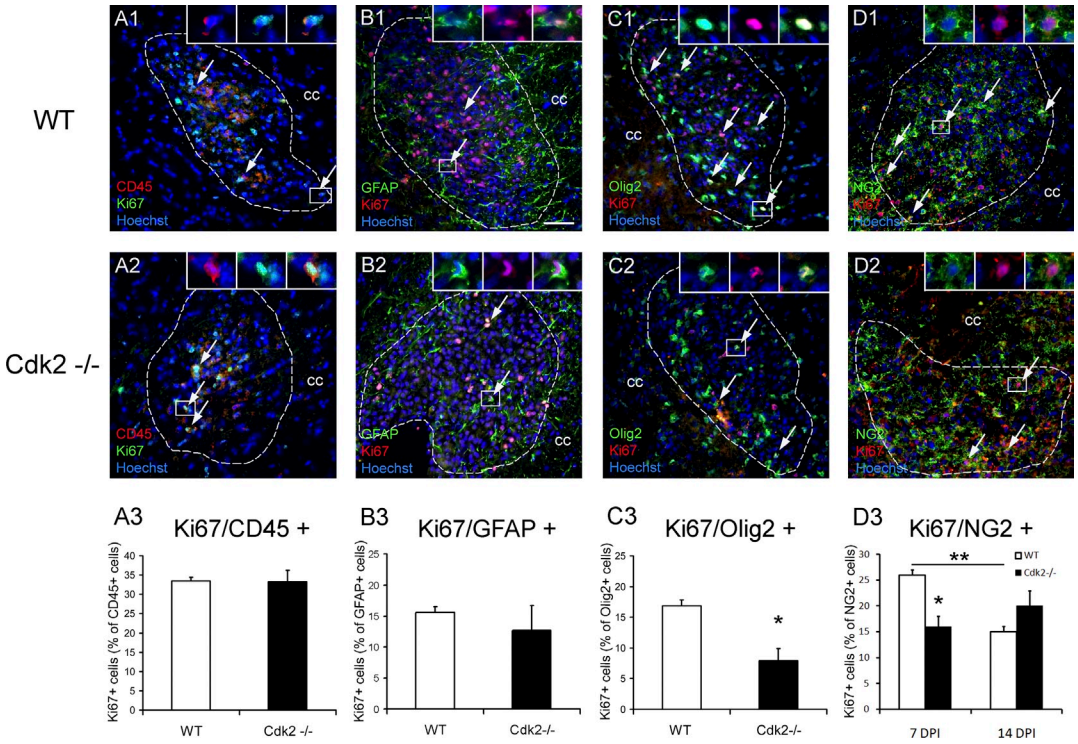

Figure 5. **Oligodendrocyte proliferation in the LPC lesion.** Characterization of proliferating cells in demyelinated lesions of the CC on sagittal sections obtained from WT (A1–D1) and Cdk2$^{-/-}$ (A2–D2) P90 mice after demyelination. Sections are stained with anti-Ki67 and a marker specific for different cell types: CD45 (A1–2) at 4 dpi, GFAP (B1–2), Olig2 (C1–2) at 7 dpi, and NG2 (D1–2) at 7 dpi and 14 dpi. Broken lines delineate the demyelinated lesion. Arrows point to double-labeled cells. Cells in the boxed areas are shown with threefold magnification in the insets. Bar, 50 µm. (A3–D3) Histograms representing the number of proliferating cells of each type in the demyelinated lesion. Results are expressed as means ± SEM (error bars; *, $P < 0.05$; **, $P < 0.001$) and were analyzed by a *t* test.

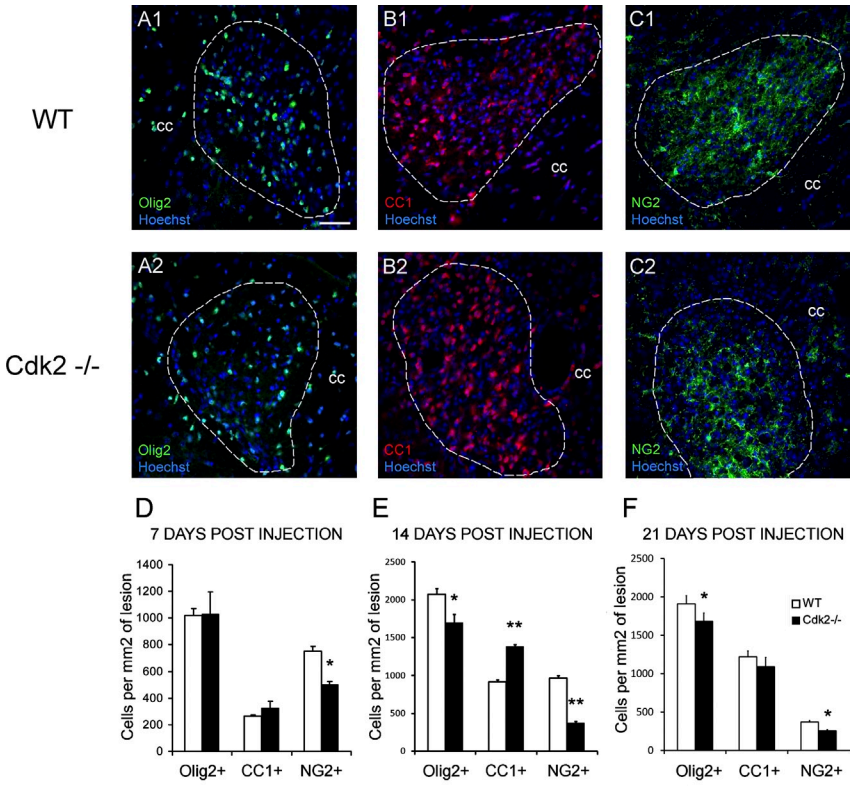

Figure 6. **Differentiation of oligodendrocytes in the absence of Cdk2.** Immunolabeling of distinct stages of oligodendroglial maturation in demyelinated lesions of the CC on sagittal sections obtained from WT (A1–C1) and Cdk2$^{-/-}$ (A2–C2) P90 mice at 14 dpi. Olig2 (A1–2) labels the overall oligodendroglia, whereas CC1 (B1–2) is specific for postmitotic oligodendrocytes, and NG2 (C1–2) identifies OPCs. Broken lines delineate the demyelinated lesion. Bar, 50 µm. (D–F) Histograms representing the number of different oligodendroglial cells/mm^2 of demyelinated lesion at 7 (D), 14 (E), and 21 (F) dpi. Results are expressed as means ± SEM (error bars; *, $P < 0.05$; **, $P < 0.001$) and were analyzed by a *t* test.

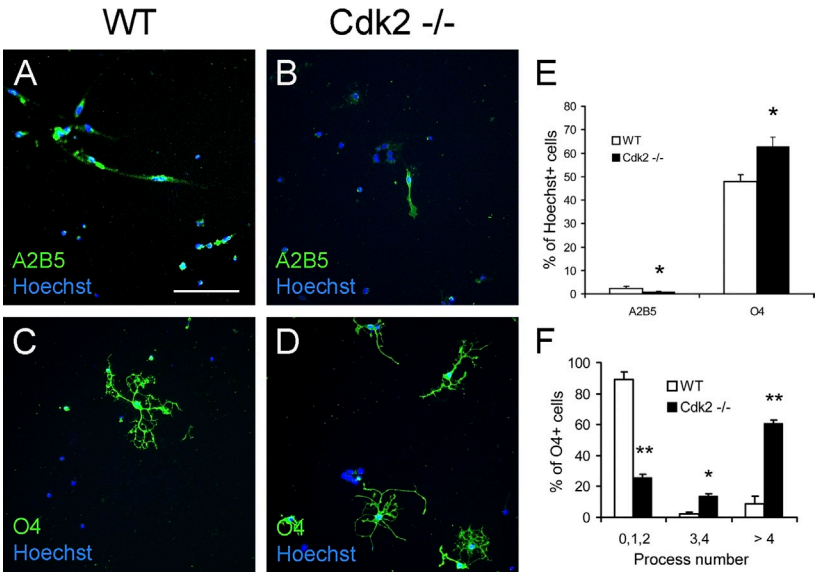

Figure 7. **Adult OPC differentiation in vitro.** After 5 d in vitro, oligodendrocytes isolated from WT (A and C) and Cdk2$^{-/-}$ (B and D) P60 mice were immunostained with anti-A2B5 (A and B) and anti-O4 (C and D). Bar, 100 µm. (E) Histogram representing the percentages of the different cell types. (F) Histogram representing the proportion of O4^{+} cells according to their process number. Results are expressed as means ± SEM (error bars; *, P < 0.05; **, P < 0.001) and were analyzed by a *t* test.

axons in the lesion at 14 dpi; i.e., at a time corresponding to a high rate of OPC differentiation into oligodendrocytes (Fig. 8 A). We found a twofold increase in the percentage of myelinated axons in the lesion of Cdk2$^{-/-}$ mice, as compared with WT (Fig. 8, B–D). Moreover, myelin thickness, as assessed by g ratio measurements, was also found to be significantly higher in the lesion of Cdk2$^{-/-}$ mice (Fig. 8 E). These differences were transient because electron microscopy analysis at 21 dpi confirmed that the delay of remyelination recovered with time in WT mice (Fig. 8, D and E), as suggested by immunohistochemical analysis (Fig. 6 F). To eliminate the possibility that differences observed at 14 dpi reflected an alteration in axon density, we quantified the number of axons in the lesion and found that the total number of axons per lesion was identical between the two genotypes (WT, 224,700 ± 19,220 axons/mm^2; Cdk2$^{-/-}$, 261,500 ± 16,180 axons/mm^2; P = 0.15; results were analyzed with a *t* test). Altogether, these data demonstrate that remyelination was accelerated in the absence of Cdk2 as a result of accelerated oligodendrocyte differentiation and decreased proliferation.

Discussion

The identification of extrinsic and intrinsic factors governing progenitor cell proliferation and differentiation in the postnatal brain is crucial to elucidate fundamental mechanisms of postnatal neurogenesis and gliogenesis. Because adult OPCs and NPCs contribute to myelin repair, identification of these factors is also crucial to understanding endogenous remyelination, which in diseases such as multiple sclerosis is insufficient to ensure definitive recovery. Although our knowledge of extracellular signals that regulate OPC and NPC cell division is quite extensive, the specific role of intrinsic regulators is less well defined. In the present study, we took advantage of a viable Cdk2$^{-/-}$ mutant mouse (Berthet et al., 2003) to investigate the functional role of this cell cycle regulator in NPC/OPC proliferation and differentiation in both normal postnatal/adult brain and after demyelination. We provide evidence that although Cdk2 loss does not affect OPC cell cycle or the normal developmental process of myelination, it clearly alters adult OPC renewal and differentiation under pathological conditions, leading to accelerated CNS remyelination.

We first analyzed Cdk2-deficient mice to elucidate the functional involvement of Cdk2 in OPC proliferation, oligodendrogenesis, and developmental myelination in vivo. Loss of Cdk2 had no effect on OPC proliferation and generation of oligodendrocytes during early postnatal (P8) development and in the adult (P90) CC. Moreover, differences in density and distribution of cells representing different stages of oligodendrocyte development were not observed in WT versus Cdk2$^{-/-}$ adult mice (P90), which suggests that Cdk2 is not required for normal development of myelinating oligodendrocytes in the postnatal and adult CNS. These data were confirmed by Western blot quantification of myelin in the early postnatal (P15) and adult

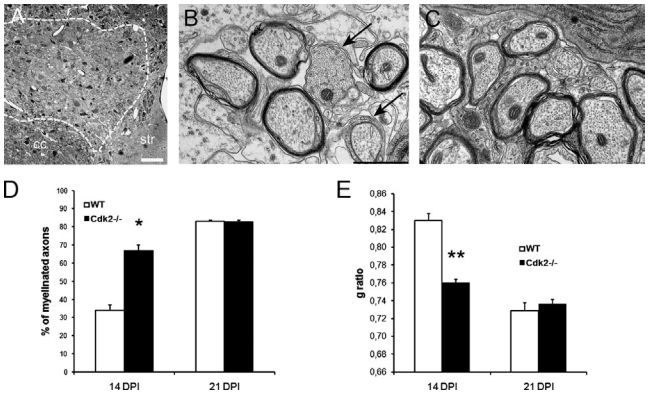

Figure 8. **Remyelination 14 and 21 d after LPC injection.** (A) Overview of a demyelinated lesion on a semithin section. Bar, 50 µm. (B and C) Images of the demyelinated lesion were taken by electron microscopy from ultrathin sections of WT (B) and Cdk2$^{-/-}$ (C) P90 mice 14 dpi. Arrows point to demyelinated axons. Bar, 1 µm. (D) Histogram representing the percentage of myelinated axons compared with the total number of axons. (E) Histogram representing the g ratio in WT versus Cdk2$^{-/-}$ mice. Results are expressed as means ± SEM (error bars; *, P < 0.05; **, P < 0.001) and were analyzed by a *t* test.

CC (P90) demonstrating similar levels of myelin protein expression in $Cdk2^{-/-}$ and WT mice. Finally, electron microscopy did not reveal changes in axonal preservation or in the number of myelinated axons, or differences in myelin structure, after Cdk2 loss in the postnatal (P15) or adult (P90) CC, as myelin compaction and g ratio did not significantly differ in $Cdk2^{-/-}$ and WT mice. Collectively, these data suggest that OPC proliferation and oligodendrogenesis during early postnatal and adult stages are either Cdk2 independent or are efficiently compensated by other Cdks.

Cdk1 could play this role, as unicellular organisms such as yeasts only require Cdk1 to drive cell division, and in the absence of interphase Cdks, Cdk1 can execute all the events that are required to drive mammalian cell division (Santamaría et al., 2007). In $p27^{-/-}$;$Cdk2^{-/-}$ double KO mice, Cdk1 compensates the loss of Cdk2 function, binding to cyclin E and regulating G1/S transition (Berthet et al., 2003). As previously suggested, Cdk4 is also a strong candidate for functional compensation of Cdk2 (Jablonska et al., 2007), as both Cdk2 and Cdk4 are activated by their regulatory proteins cyclin E and D, respectively, to sequentially phosphorylate Rb. Although $Cdk2^{-/-}$ or $Cdk4^{-/-}$ mice are viable, $Cdk2^{-/-}$;$Cdk4^{-/-}$ double KO mice die in utero around embryonic day 15 (E15; Berthet et al., 2006). Moreover, elevated levels of Cdk4 protein expression and activity were observed in $Cdk2^{-/-}$ tissue up to P15, before declining with comparable levels to WT mice (Jablonska et al., 2007). Consistent with this finding, proliferation and self-renewal of NPCs in the adult SVZ were indistinguishable in $Cdk2^{-/-}$ and WT mice up to P15 and then reduced in the adult (Jablonska et al., 2007). Therefore, the lack of significant differences in developmental myelination between $Cdk2^{-/-}$ and WT mice are likely to result from compensatory mechanisms occurring during CNS development.

Although OPCs are still produced in the adult from SVZ cells (Menn et al., 2006; Dimou et al., 2008; Rivers et al., 2008), decreased proliferation of these cells under physiological conditions in the absence of Cdk2 (Jablonska et al., 2007; this study) seems sufficient to maintain a normal density of oligodendroglial cells in the CC. However, when challenged with demyelination, a process known to enhance proliferation of resident adult OPCs and SVZ precursors (Nait-Oumesmar et al., 1999; Decker et al., 2002), we found that cell proliferation was reduced not only in the SVZ, but also in the lesion of $Cdk2^{-/-}$ mice. These alterations were not an indirect consequence of axonal loss, as no obvious alterations in axons and/or in axonal density were observed by electron microscopy. However, we cannot presently fully exclude the possibility that disruption of Cdk2 function could have enhanced cell recruitment to the lesion, thereby eliminating the need for self-renewal of local progenitors. This could have resulted in decreased OPC proliferation observed in the lesion of $Cdk2^{-/-}$ mice.

Because decreased proliferation specifically affected cells giving rise to oligodendrocytes, including OPCs and type C cells of the SVZ, rather than microglia and astrocytes, we investigated the consequences of altered proliferation on OPC differentiation into oligodendrocytes. We showed that reduced proliferation was correlated with enhanced cell cycle exit in adult OPCs of $Cdk2^{-/-}$ mice, as compared with WT, as well as with enhanced differentiation of adult OPCs into differentiated $CC1^+$ oligodendrocytes. Interestingly, although $NG2^+$ OPC densities were identical in the CC of WT and $Cdk2^{-/-}$ noninjured mice, their reduced proliferation at 7 dpi coincided with a reduction in OPC density in $Cdk2^{-/-}$ mice as compared with WT. In contrast, $CC1^+$ oligodendrocyte density increased in $Cdk2^{-/-}$ mice 1 and 2 wk later, a delay corresponding to the onset of remyelination and the oligodendrocyte/myelin regeneration period in LPC lesions, respectively. However, differences between $Cdk2^{-/-}$ mice and WT disappeared by 21 d, when the process of repair was nearly accomplished. Moreover, we demonstrate that increased cell cycle exit and oligodendrocyte differentiation in $Cdk2^{-/-}$ mice had a direct impact on the number of remyelinated axons, and on the extent of axonal remyelination, as assessed by g ratio measurements in the lesion. The fact that remyelination in WT mice leveled with that of $Cdk2^{-/-}$ mice at 21 dpi further underlines the fact that Cdk2 acts as a modulator rather than as an on/off switch of the differentiation/remyelination process. These results are consistent with previous in vitro findings showing that Cdk2 loss decreased OPC proliferation (Belachew et al., 2002) and promoted lineage commitment of NG2-expressing progenitors in the adult SVZ, and differentiation of adult neural progenitor cells (Jablonska et al., 2007). As the consequences of Cdk2 loss on adult OPC differentiation have not yet been described, this study highlights for the first time the role of Cdk2 as an intrinsic molecular mechanism that controls the timing of oligodendrocyte differentiation in vivo. This conclusion is supported by our findings that accelerated differentiation of oligodendroglial cells in the absence of Cdk2 also occurred in vitro.

The role of Cdk2 in proliferation of adult hippocampal neural progenitors was also previously investigated. Interestingly, in this progenitor population, Cdk2 did not appear to play a crucial role in cell proliferation, even after induction of seizures (Vandenbosch et al., 2007). This discrepancy could be explained by compensatory mechanisms, which may be region-specific and may reflect the low proliferative potential of hippocampal progenitors, as compared with their SVZ counterpart. Alternatively, these differences may have resulted from a nonessential role played by Cdk2 in neurogenic regions of the brain, such as the adult hippocampus, as compared with the SVZ, which is directly involved in oligodendrogenesis, a process that more closely depends on the control of OPC proliferation by Cdk2.

In conclusion, the requirement for Cdk2 appears to be time, region, and cell specific. Despite the redundant function of Cdk2 in development, as demonstrated by the finding that $Cdk2^{-/-}$ mice are viable and display normal myelination, the present study reveals a crucial role for Cdk2 in adult OPC/NPC proliferation under pathological conditions. These findings could contribute to a better understanding of remyelination failure in multiple sclerosis. In this inflammatory disease, endogenous remyelination exists but is not efficient in all lesions. Among several possible hypotheses, dysregulation of OPC proliferation has been proposed to play a role in remyelination failure, as demonstrated by reduced OPC proliferation in some lesions, although in others OPCs are numerous, but appear unable to

fully differentiate (Chang et al., 2002). A previous study also demonstrated that persistent CNS inflammation significantly altered cell kinetics of precursors and stem cells in experimental autoimmune encephalomyelitis, a model of multiple sclerosis (Pluchino et al., 2008). In view of the role of Cdk2 described here in adult NPCs/OPCs, altered proliferation or differentiation of these cells in multiple sclerosis could be related to Cdk2 dysregulation and could be, at least in part, responsible for the observed failure in remyelination. Thus, our study not only contributes to a better understanding of NPC/OPC cell cycle control and expansion versus differentiation under normal physiological conditions, but demonstrates a specific role of Cdk2 in remyelination, which may be crucial to design novel therapeutic approaches to promote CNS remyelination.

Materials and methods

Animals

Cdk2 mutant mice were generated by replacing exons 4 and 5 encoding the core kinase domain of Cdk2 with a PGK-neomycin cassette to functionally inactivate the Cdk2 gene (Berthet et al., 2003). This line was kept under a mixed background (C57BL/6 × 129S7/SvlmJ × CD1) as Cdk2 heterozygotes because $Cdk2^{-/-}$ males and females are sterile. Early postnatal (P8 and P15) or adult (P90) WT and $Cdk2^{-/-}$ littermates were used in all experiments. Mice were group-housed under standard conditions with food and water available ad libitum, and were maintained on a 12 h light/dark cycle. All animal protocols were performed in accordance with the guidelines published in the National Institutes of Health Guide for the Care and Use of Laboratory Animals.

Focal LPC-induced demyelination

As described previously (Nait-Oumesmar et al., 1999), five adult animals (P90) of each genotype were deeply anesthetized with 100 mg/kg body weight ketamine (Imalgene) and 10 mg/kg body weight xylazine (Rompun) dissolved in 0.9% sterile saline, and positioned in a stereotaxic frame. Animals were injected unilaterally into the CC, using appropriate coordinates (1.5 mm anterior to the bregma, 1 mm lateral and 1.8 mm deep from the skull surface) with 2 µl of a 1% LPC solution (Sigma-Aldrich) in 0.9% NaCl. Animals were sacrificed 7, 14, and 21 d after LPC injection.

Cell proliferation

Cell proliferation was assessed by using Ki67 and/or BrdU immunostaining. To assay proliferation in response to demyelination, at 7 d after LPC injection, two intraperitoneal injections of BrdU (60 mg/kg body weight; Sigma-Aldrich) were performed at 2-h intervals on the day of sacrifice. Animals were sacrificed at 2 h after the last BrdU injection.

Tissue processing for immunohistochemistry

P8, P15, and P90 animals were anesthetized with a lethal dose of ketamine (Imalgene) and intracardially perfused with 4% PFA in cold 0.1 M phosphate buffer (PBS, pH 7.4), and brains were postfixed in the same fixative for 1 h. Fixed tissues were then cryoprotected in 20% sucrose overnight at 4°C, and finally frozen at −60°C in isopentane cooled by liquid N_2.

12-µm sagittal sections were cut with a cryostat (CM 3050S; Leica) and stored at −20°C for immunohistochemistry.

Immunohistochemistry

Sections were incubated at RT for 20 min in blocking solution (PBS containing 0.1% Triton X-100 and 10% normal goat serum). Primary antibodies were diluted using the same carrier solution and incubated overnight at 4°C. Primary antibody dilutions were 1:100 for rabbit polyclonal anti-Olig2 (Millipore), rabbit polyclonal anti-NG2 (Abcys SA), mouse monoclonal anti-APC (clone CC1) designated here as anti-CC1 (EMD), mouse monoclonal anti-MAG (Millipore), mouse monoclonal anti-CNPase (Millipore), mouse monoclonal anti-Mash1 (BD), mouse monoclonal anti-PSA-NCAM (AbCys SA), rabbit polyclonal anti-GFAP (Dako), rabbit polyclonal anti-MBP (Millipore), rat monoclonal anti-CD45 (Invitrogen), and mouse monoclonal anti-Ki67 (BD).

Sections were washed and incubated for 1 h with species-specific secondary antibodies conjugated to FITC or TRITC (SouthernBiotech or Dako) diluted at 1:100 in carrier solution. Nuclei were counterstained with the nucleic acid stain Hoechst 33342 (Sigma-Aldrich) diluted at 1:1,000 in PBS. Finally, tissue sections were washed in PBS and mounted under coverslips using Fluoromount (SouthernBiotech).

Immunohistochemistry for BrdU was performed treating sections for 30 min at 37°C with HCl 2 N in PBS containing 0.1% Triton X-100, then rinsed two times in 0.1 M sodium tetraborate buffer, pH 8.5. After several washes in PBS, sections were incubated overnight at 4°C with rat monoclonal anti-BrdU antibody (1:100; AbCys SA). For double labeling, sections were first immunostained with antibodies as just described, then postfixed for 15 min in PFA 4% before BrdU pretreatment and labeling.

In vitro differentiation of adult OPC

Brains from 6 adult (P60) animals of each genotype were dissected and enzymatically digested using a solution containing 240 µg/ml L-cysteine, 1.2 U/ml papain, and 40 µg/ml DNase (Sigma-Aldrich) at 37°C in a shaking water bath during 1 h. Tissue was then triturated with a Pasteur pipet and filtered through 40-µm mesh. Dissociated cells were layered on a performed Percoll gradient at 23,500 *g* for 20 min (GE Healthcare). The fraction containing glial progenitors and localized between the myelin and red blood cell fractions was then recovered. After washing, cells were resuspended in N1 (DME supplemented with insulin, transferrin, progesterone, putrescine, and selenium; Invitrogen and Sigma-Aldrich), a serum-free medium mixed with B104 conditioned medium to increase the proportion of oligodendrocyte progenitors. Cells were plated in 4-well plates coated with polyornithine/laminin (Sigma-Aldrich) at 10^5 cells/well and kept at 37°C in a humidified 9% CO_2/air atmosphere.

Immunocytochemical analysis of specific cell markers was performed at 5 h and 5 d after plating.

Tissue processing for electron microscopy

Unlesioned animals were sacrificed for analysis at P15 or P90, and adult lesioned mice were sacrificed 14 and 21 d after LPC injection. Animals were intracardially perfused with 2% PFA and 2.5% glutaraldehyde (Electron Microscopy Sciences) in 0.1 M phosphate buffer. Lesioned brains were removed and cut into 100-µm free-floating vibratome sections (VT 1000S; Leica). Slices were then postfixed with 2.5% glutaraldehyde for 2 h and 2% osmium tetroxide (Electron Microscopy Sciences) for 30 min. After dehydration, slices were flat-embedded in epon. Ultrathin sections of the area of interest were cut using an ultramicrotome (Ultracut E; Reichert-Jung) and were analyzed using an electron microscope (CM 120; Philips).

Western blotting

Slices of 700 µm were cut out with a vibratome from P15 and P90 brains before the CC was carefully microdissected. Protein extraction was performed using RIPA lysis buffer (50 mM Tris-HCl, pH 7.5, 1 mM EDTA, 1 mM EGTA, 1 mM sodium orthovanadate, 50 mM sodium fluoride, 0.1% 2-mercaptoethanol, 1% Triton X-100, and proteases inhibitor cocktail). Protein concentration was determined in each sample. Protein extracts were boiled for 5 min before loading onto 4–20% gradient gels (GeneMate; Bioexpress; 20 µg of protein per each lane). Gels were electrotransferred to a 0.2 µm nitrocellulose membrane (Millipore). Blots were blocked in 5% milk in TBST for 1 h, and then incubated at 4°C overnight with one of the following antibodies: anti-MBP (Covance) and anti-actin (Millipore). Bands were detected with appropriate horseradish peroxide–conjugated secondary antibodies, reacted with chemiluminescent ECL substrate (GE Healthcare), and visualized by exposure to x rays. Band intensity was measured using the ImageJ 1.39o software (National Institutes of Health). Western blots were obtained from the CC of 3–4 different animals in each group and age. Data were averaged and were represented as means ± SEM.

Quantification and statistical analyses

For quantitative data in unlesioned animals (4–5 animals/group), three sections were selected, 120 µm apart, with a starting point corresponding to the most rostral crossing of the CC. For each section, two to three fields were acquired in the medial part of the CC (5 µm thickness; step size = 1 µm between successive images of the same field) with a 60× objective lens using a confocal system (Fluoview FV1000; Olympus) equipped with an inverted microscope (IX81; Olympus). Corresponding images were quantified using the FV10-ASW software (Olympus) and cell counts were expressed as the number of cells per volume (10^4 µm^3) of CC. Statistical analysis was performed using unpaired two-tailed *t* test (Prism software, version 4.00; GraphPad Software Inc.).

For quantitative data in demyelinated animals (4–5 animals/group unless indicated), labeled cells were counted in the lesion previously identified by MBP immunolabeling. Cells were counted in the entire lesion area (two to four 12-µm sagittal sections through the CC), and results were expressed as number of cells per area of lesion (mm^2). In the anterior subventricular zone (six 12-µm sagittal sections), results were expressed as the number of cells per surface (mm^2). Images were acquired with a 40× objective lens using a fluorescent microscope (DBM; Leica) and image acquisition software (Explora Nova). Corresponding images were quantified using the ImageJ 1.39o software. Statistical analysis was performed using unpaired two-tailed *t* test (SigmaStat for Windows version 3.11; Systat Software Inc.).

For quantification by electron microscopy of P15 and P90 unlesioned brains or adult brains, 14 and 21 d after LPC injection (3–4 per group), 15–20 electron microscope fields were randomly taken in the CC or in the lesion area at a magnification of 9,700. For unlesioned brain analysis, the numbers of total axons and myelinated axons were counted and expressed as a number of axons or myelinated axons per surface (mm^2). For lesioned brain analysis, the numbers of myelinated and unmyelinated axons in the lesion were counted. The percentage of myelinated axons was expressed as the percentage of the total number of axons in the lesion, and the total number of axons in the lesion was expressed as a number of axons per surface (mm^2). The g ratio in nonlesioned CC and in the lesion was obtained by dividing axon circumference by axon plus myelin sheath circumference measured using the ImageJ 1.39o software at a magnification of 33,000 magnification. Statistical analysis was performed using unpaired two-tailed *t* test (SigmaStat).

Evaluation of cell death with TUNEL assay

Apoptotic nuclei were labeled in situ by the TUNEL method (Promega). Frozen sections of fixed tissue were brought to RT, rinsed for 5 min in PBS twice, and treated with 20 µg/ml proteinase K for 10 min at RT to permeabilize tissues to the staining reagents. After a 5-min rinse in PBS, sections were fixed for 5 min with PFA 4% at RT. After PBS rinsing, sections were preincubated in equilibration buffer (25 mM Tris-HCl, pH 6.6, containing 200 mM potassium cacodylate and 2.5 mM cobalt chloride). Sections were then drop-incubated in TdT incubation buffer (containing rTdT enzyme and 5 µM fluorescein-12-dUTP) in a humidified chamber for 60 min at 37°C. The reaction was stopped by a 15-min immersion in 2× SSC buffer (300 mM NaCl and 30 mM sodium citrate). Sections were rinsed three times in PBS to remove unincorporated fluorescein-12-dUTP. As described previously, nuclei were counterstained with Hoechst 33342 (Sigma-Aldrich), and tissue sections were mounted under coverslips using Fluoromount (SouthernBiotech).

Online supplemental material

Fig. S1 shows that there is no difference comparing oligodendroglial lineage in the CC area from WT and $Cdk2^{-/-}$ mice. Fig. S2 shows that there is no difference comparing OPC proliferation and myelination from WT and $Cdk2^{-/-}$ P90 mice. Fig. S3 shows that cell proliferation assessed by BrdU in response to demyelination in the adult brain is decreased in $Cdk2^{-/-}$ mice compared with WT mice. Fig. S4 shows that there is no difference in apoptosis in response to demyelination comparing WT and $Cdk2^{-/-}$ P90 mice. Fig. S5 shows that proliferation of $GFAP^+$ and $PSA\text{-}NCAM^+$ cells from the adult ASVZ is not affected by the loss of Cdk2 in response to demyelination. Online supplemental material is available at http://www.jcb.org/cgi/content/full/jcb.201004146/DC1.

We thank Drs. B. Nait-Oumesmar, V. Zujovic, and V. Tepavcevic for fruitful discussions; Dr. Ph. Kaldis for giving us access to Cdk2 mutant mice; and Dr. P. Beukelaers for genotyping mice from Belgium. We are grateful to Dr. D. Langui (Imaging Platform at Salpêtrière Hospital) and Dr. C. Bachelin for precious technical assistance on electron microscopy.

This work was supported by grants from the European Leukodystrophy Association Foundation (to A. Baron-Van Evercooren, V. Gallo, and B. Malgrange), Institut National de la Santé et de la Recherche Médicale (A. Baron-Van Evercooren), Fonds Léon Frédericq (to B. Malgrange), and from the National Institutes of Health (R01NS045702 to V. Gallo) and National Institutes of Health Duke Training Program in Clinical Research (P30HD40677 to V. Gallo). C. Caillava and G. Spigoni were supported by fellowships from the European Leukodystrophy Association Foundation. B. Malgrange is senior research associate of the Fonds de la Recherche Scientifique. A. Baron-Van Evercooren benefits from a Contrat d'Interface AP-HP.

Submitted: 28 April 2010
Accepted: 24 March 2011

References

Aguirre, A.A., R. Chittajallu, S. Belachew, and V. Gallo. 2004. NG2-expressing cells in the subventricular zone are type C-like cells and contribute to interneuron generation in the postnatal hippocampus. *J. Cell Biol.* 165:575–589. doi:10.1083/jcb.200311141

Aguirre, A., J.L. Dupree, J.M. Mangin, and V. Gallo. 2007. A functional role for EGFR signaling in myelination and remyelination. *Nat. Neurosci.* 10:990–1002. doi:10.1038/nn1938

Atanasoski, S., M. Boentert, L. De Ventura, H. Pohl, C. Baranek, K. Beier, P. Young, M. Barbacid, and U. Suter. 2008. Postnatal Schwann cell proliferation but not myelination is strictly and uniquely dependent on cyclin-dependent kinase 4 (cdk4). *Mol. Cell. Neurosci.* 37:519–527. doi:10.1016/j.mcn.2007.11.005

Belachew, S., A.A. Aguirre, H. Wang, F. Vautier, X. Yuan, S. Anderson, M. Kirby, and V. Gallo. 2002. Cyclin-dependent kinase-2 controls oligodendrocyte progenitor cell cycle progression and is downregulated in adult oligodendrocyte progenitors. *J. Neurosci.* 22:8553–8562.

Berthet, C., E. Aleem, V. Coppola, L. Tessarollo, and P. Kaldis. 2003. Cdk2 knockout mice are viable. *Curr. Biol.* 13:1775–1785. doi:10.1016/j.cub.2003.09.024

Berthet, C., K.D. Klarmann, M.B. Hilton, H.C. Suh, J.R. Keller, H. Kiyokawa, and P. Kaldis. 2006. Combined loss of Cdk2 and Cdk4 results in embryonic lethality and Rb hypophosphorylation. *Dev. Cell.* 10:563–573. doi:10.1016/j.devcel.2006.03.004

Boggs, J.M. 2006. Myelin basic protein: a multifunctional protein. *Cell. Mol. Life Sci.* 63:1945–1961. doi:10.1007/s00018-006-6094-7

Cerghet, M., R.P. Skoff, D. Bessert, Z. Zhang, C. Mullins, and M.S. Ghandour. 2006. Proliferation and death of oligodendrocytes and myelin proteins are differentially regulated in male and female rodents. *J. Neurosci.* 26:1439–1447. doi:10.1523/JNEUROSCI.2219-05.2006

Chang, A., A. Nishiyama, J. Peterson, J. Prineas, and B.D. Trapp. 2000. NG2-positive oligodendrocyte progenitor cells in adult human brain and multiple sclerosis lesions. *J. Neurosci.* 20:6404–6412.

Chang, A., W.W. Tourtellotte, R. Rudick, and B.D. Trapp. 2002. Premyelinating oligodendrocytes in chronic lesions of multiple sclerosis. *N. Engl. J. Med.* 346:165–173. doi:10.1056/NEJMoa010994

Decker, L., N. Picard-Riera, F. Lachapelle, and A. Baron-Van Evercooren. 2002. Growth factor treatment promotes mobilization of young but not aged adult subventricular zone precursors in response to demyelination. *J. Neurosci. Res.* 69:763–771. doi:10.1002/jnr.10411

Dimou, L., C. Simon, F. Kirchhoff, H. Takebayashi, and M. Götz. 2008. Progeny of Olig2-expressing progenitors in the gray and white matter of the adult mouse cerebral cortex. *J. Neurosci.* 28:10434–10442. doi:10.1523/JNEUROSCI.2831-08.2008

Doetsch, F., I. Caillé, D.A. Lim, J.M. García-Verdugo, and A. Alvarez-Buylla. 1999. Subventricular zone astrocytes are neural stem cells in the adult mammalian brain. *Cell.* 97:703–716. doi:10.1016/S0092-8674(00)80783-7

Doetsch, F., J.M. Verdugo, I. Caille, A. Alvarez-Buylla, M.V. Chao, and P. Casaccia-Bonnefil. 2002. Lack of the cell-cycle inhibitor p27Kip1 results in selective increase of transit-amplifying cells for adult neurogenesis. *J. Neurosci.* 22:2255–2264.

Ffrench-Constant, C., and M.C. Raff. 1986. Proliferating bipotential glial progenitor cells in adult rat optic nerve. *Nature*. 319:499–502. doi:10.1038/319499a0

Fields, R.D. 2008. White matter in learning, cognition and psychiatric disorders. *Trends Neurosci.* 31:361–370. doi:10.1016/j.tins.2008.04.001

Franklin, R.J. 2002. Why does remyelination fail in multiple sclerosis? *Nat. Rev. Neurosci.* 3:705–714. doi:10.1038/nrn917

Gensert, J.M., and J.E. Goldman. 1997. Endogenous progenitors remyelinate demyelinated axons in the adult CNS. *Neuron*. 19:197–203. doi:10.1016/S0896-6273(00)80359-1

Jablonska, B., A. Aguirre, R. Vandenbosch, S. Belachew, C. Berthet, P. Kaldis, and V. Gallo. 2007. Cdk2 is critical for proliferation and self-renewal of neural progenitor cells in the adult subventricular zone. *J. Cell Biol.* 179:1231–1245. doi:10.1083/jcb.200702031

Lange, C., W.B. Huttner, and F. Calegari. 2009. Cdk4/cyclinD1 overexpression in neural stem cells shortens G1, delays neurogenesis, and promotes the generation and expansion of basal progenitors. *Cell Stem Cell*. 5:320–331. doi:10.1016/j.stem.2009.05.026

Levison, S.W., and J.E. Goldman. 1993. Both oligodendrocytes and astrocytes develop from progenitors in the subventricular zone of postnatal rat forebrain. *Neuron*. 10:201–212. doi:10.1016/0896-6273(93)90311-E

Malumbres, M., R. Sotillo, D. Santamaría, J. Galán, A. Cerezo, S. Ortega, P. Dubus, and M. Barbacid. 2004. Mammalian cells cycle without the D-type cyclin-dependent kinases Cdk4 and Cdk6. *Cell*. 118:493–504. doi:10.1016/j.cell.2004.08.002

Matthews, M.A., and D. Duncan. 1971. A quantitative study of morphological changes accompanying the initiation and progress of myelin production in the dorsal funiculus of the rat spinal cord. *J. Comp. Neurol.* 142:1–22. doi:10.1002/cne.901420102

Menn, B., J.M. Garcia-Verdugo, C. Yaschine, O. Gonzalez-Perez, D. Rowitch, and A. Alvarez-Buylla. 2006. Origin of oligodendrocytes in the subventricular zone of the adult brain. *J. Neurosci.* 26:7907–7918. doi:10.1523/JNEUROSCI.1299-06.2006

Moons, D.S., S. Jirawatnotai, A.F. Parlow, G. Gibori, R.D. Kineman, and H. Kiyokawa. 2002. Pituitary hypoplasia and lactotroph dysfunction in mice deficient for cyclin-dependent kinase-4. *Endocrinology*. 143:3001–3008. doi:10.1210/en.143.8.3001

Morgan, D.O. 1997. Cyclin-dependent kinases: engines, clocks, and microprocessors. *Annu. Rev. Cell Dev. Biol.* 13:261–291. doi:10.1146/annurev.cellbio.13.1.261

Nait-Oumesmar, B., L. Decker, F. Lachapelle, V. Avellana-Adalid, C. Bachelin, and A.B. Van Evercooren. 1999. Progenitor cells of the adult mouse subventricular zone proliferate, migrate and differentiate into oligodendrocytes after demyelination. *Eur. J. Neurosci.* 11:4357–4366. doi:10.1046/j.1460-9568.1999.00873.x

Nait-Oumesmar, B., N. Picard-Riera, C. Kerninon, L. Decker, D. Seilhean, G.U. Höglinger, E.C. Hirsch, R. Reynolds, and A. Baron-Van Evercooren. 2007. Activation of the subventricular zone in multiple sclerosis: evidence for early glial progenitors. *Proc. Natl. Acad. Sci. USA*. 104:4694–4699. doi:10.1073/pnas.0606835104

Nishiyama, A. 1998. Glial progenitor cells in normal and pathological states. *Keio J. Med.* 47:205–208.

Nishiyama, A. 2007. Polydendrocytes: NG2 cells with many roles in development and repair of the CNS. *Neuroscientist*. 13:62–76. doi:10.1177/1073858406295586

Ortega, S., I. Prieto, J. Odajima, A. Martín, P. Dubus, R. Sotillo, J.L. Barbero, M. Malumbres, and M. Barbacid. 2003. Cyclin-dependent kinase 2 is essential for meiosis but not for mitotic cell division in mice. *Nat. Genet.* 35:25–31. doi:10.1038/ng1232

Parras, C.M., C. Hunt, M. Sugimori, M. Nakafuku, D. Rowitch, and F. Guillemot. 2007. The proneural gene Mash1 specifies an early population of telencephalic oligodendrocytes. *J. Neurosci.* 27:4233–4242. doi:10.1523/JNEUROSCI.0126-07.2007

Pfeiffer, S.E., A.E. Warrington, and R. Bansal. 1993. The oligodendrocyte and its many cellular processes. *Trends Cell Biol.* 3:191–197. doi:10.1016/0962-8924(93)90213-K

Picard-Riera, N., L. Decker, C. Delarasse, K. Goude, B. Nait-Oumesmar, R. Liblau, D. Pham-Dinh, and A.B. Evercooren. 2002. Experimental autoimmune encephalomyelitis mobilizes neural progenitors from the subventricular zone to undergo oligodendrogenesis in adult mice. *Proc. Natl. Acad. Sci. USA*. 99:13211–13216. doi:10.1073/pnas.192314199

Pluchino, S., L. Muzio, J. Imitola, M. Deleidi, C. Alfaro-Cervello, G. Salani, C. Porcheri, E. Brambilla, F. Cavasinni, A. Bergamaschi, et al. 2008. Persistent inflammation alters the function of the endogenous brain stem cell compartment. *Brain*. 131:2564–2578. doi:10.1093/brain/awn198

Rane, S.G., P. Dubus, R.V. Mettus, E.J. Galbreath, G. Boden, E.P. Reddy, and M. Barbacid. 1999. Loss of Cdk4 expression causes insulin-deficient diabetes and Cdk4 activation results in beta-islet cell hyperplasia. *Nat. Genet.* 22:44–52. doi:10.1038/8751

Reynolds, R., and R. Hardy. 1997. Oligodendroglial progenitors labeled with the O4 antibody persist in the adult rat cerebral cortex in vivo. *J. Neurosci. Res.* 47:455–470. doi:10.1002/(SICI)1097-4547(19970301)47:5<455::AID-JNR1>3.0.CO;2-G

Rivers, L.E., K.M. Young, M. Rizzi, F. Jamen, K. Psachoulia, A. Wade, N. Kessaris, and W.D. Richardson. 2008. PDGFRA/NG2 glia generate myelinating oligodendrocytes and piriform projection neurons in adult mice. *Nat. Neurosci.* 11:1392–1401. doi:10.1038/nn.2220

Santamaría, D., C. Barrière, A. Cerqueira, S. Hunt, C. Tardy, K. Newton, J.F. Cáceres, P. Dubus, M. Malumbres, and M. Barbacid. 2007. Cdk1 is sufficient to drive the mammalian cell cycle. *Nature*. 448:811–815. doi:10.1038/nature06046

Temple, S., and M.C. Raff. 1986. Clonal analysis of oligodendrocyte development in culture: evidence for a developmental clock that counts cell divisions. *Cell*. 44:773–779. doi:10.1016/0092-8674(86)90843-3

Tsutsui, T., B. Hesabi, D.S. Moons, P.P. Pandolfi, K.S. Hansel, A. Koff, and H. Kiyokawa. 1999. Targeted disruption of CDK4 delays cell cycle entry with enhanced p27(Kip1) activity. *Mol. Cell. Biol.* 19:7011–7019.

Vandenbosch, R., L. Borgs, P. Beukelaers, A. Foidart, L. Nguyen, G. Moonen, C. Berthet, P. Kaldis, V. Gallo, S. Belachew, and B. Malgrange. 2007. CDK2 is dispensable for adult hippocampal neurogenesis. *Cell Cycle*. 6:3065–3069. doi:10.4161/cc.6.24.5048

Watanabe, M., Y. Toyama, and A. Nishiyama. 2002. Differentiation of proliferated NG2-positive glial progenitor cells in a remyelinating lesion. *J. Neurosci. Res.* 69:826–836. doi:10.1002/jnr.10338

Wolswijk, G., and M. Noble. 1989. Identification of an adult-specific glial progenitor cell. *Development*. 105:387–400.

Woodruff, R.H., and R.J. Franklin. 1999. Demyelination and remyelination of the caudal cerebellar peduncle of adult rats following stereotaxic injections of lysolecithin, ethidium bromide, and complement/anti-galactocerebroside: a comparative study. *Glia*. 25:216–228. doi:10.1002/(SICI)1098-1136(19990201)25:3<216::AID-GLIA2>3.0.CO;2-L

Zhou, Q., S. Wang, and D.J. Anderson. 2000. Identification of a novel family of oligodendrocyte lineage-specific basic helix-loop-helix transcription factors. *Neuron*. 25:331–343. doi:10.1016/S0896-6273(00)80898-3\